International Journal of Railway Research, Vol. 6, No. 2, (2019), 1-11

Iran University of Science and Technology

International Journal of

Railway Research

ISSN: 2423-3838

A Methodology for Analyzing the Lateral Train-Structure Interaction: Application in Two Case Studies

Pedro Aires Montenegro [1], Rui Calçada[2*]

[1,2]CONSTRUCT - LESE, Faculty of Engineering, University of Porto, 4200-465 Porto, Portugal

ARTICLE INFO

Article history:
Received: 21.08.2019
Accepted: 15.10.2019
Published: 24.12.2019

Keywords:
Train-structure interaction
Bridge dynamics
Running safety
Wheel-rail contact
Earthquakes
Crosswinds

A B S T R A C T

A methodology for analyzing the lateral train-structure interaction is proposed in this article. The wheel-rail contact formulation incorporated in the methodology consists in three main steps: the geometrical problem, where the contact point position is detected; the normal contact problem, in which the forces are determined based on the Hertz theory, and the tangential contact problem, where the creep forces are calculated using the rolling friction laws proposed by Kalker. Two application cases are presented related to the running safety assessment of a train moving over bridges subjected to earthquakes and crosswinds. The dynamic response of both the bridges and the train are discussed and the running safety is assessed using criteria existent in the literature.

1. Introduction

In more recent years, the dynamic effects produced by moving trains over bridges have been becoming an important issue in the railway engineering. With the continuous increase of the operating speeds and bridge dimensions, such dynamic effects can no longer be accurately accessed with simple models based on moving loads. Therefore, the consideration of the vehicle-bridge interaction becomes relevant to access not only the dynamic effects on bridges but also the comfort and running safety of railway traffic. The development of new high-speed railway networks around the world lead to the necessity of ensuring smoother tracks with larger curve radius that resulted in railway lines with a high percentage of viaducts and bridges. Some of these bridges are situated in regions prone to earthquakes or in deep valleys, in which strong crosswinds are frequent. This reality led to new concerns among the railway engineering community, since it may represent an additional risk factor for the trains. Therefore, events such as the derailments that occurred during the Kobe Earthquake, in January 1995, the Shinkansen high-speed train derailment at 200 km/h during the Mid-Niigata Earthquake, in October 2004, or the train derailments caused by strong crosswinds reported in [1], provided the impetus for analyzing the running safety of trains moving on bridges. The train-structure interaction models vary in terms of complexity, from models that account only the vertical dynamics, in both time domain [2] and frequency domain [3], to models that also include the lateral effects [4, 5]. The latter are particularly important to study the running safety of trains subjected to lateral vibrations caused by earthquakes [6, 7] or crosswinds [8, 9]. In the present paper, an extension of the formulation described in [10] that takes into account the lateral dynamic effects between railway vehicles and structures is proposed [11]. The

*Corresponding author, Professor of Civil Eng., orcid.org/0000-0002-2375-7685
Email: ruiabc@fe.up.pt

[DOI: 10.22068/IJRARE.6.2.1]

methodology has been implemented in MATLAB [12] being the vehicles and structure modeled with ANSYS [13]. Two case studies in which the proposed methodology is applied are presented. The first application case consists of a study regarding the running safety of a high-speed train moving over a viaduct subjected to moderate earthquakes [14]. The main objective of the study consists of evaluating the influence of the earthquake intensity, track quality and train speed in the train running safety using criteria existent in the literature.

The second application is related to the assessment of the train behavior running over a high-speed railway bridge subjected to strong crosswinds. The wind is modeled through a simple but effective approach based on the discrete gust Chinese Hat model that avoids the generation of complex stochastic wind data. The dynamic responses of both bridge and vehicle are evaluated and discussed, as well as the values for the safety criteria obtained in each analysis.

2. Train-structure interaction method

2.1. Geometrical contact problem

To determine the location of the potential contact points between the wheel and rail, the following set of nonlinear equations is used

$$\begin{cases} \mathbf{t}_{r,y}^{t} \cdot \mathbf{d}_{wr}^{t} = 0 \\ \mathbf{t}_{w,y}^{t} \cdot \mathbf{n}_{r}^{t} = 0 \end{cases} \quad (1)$$

where $\mathbf{t}_{r,y}^{t}$ and $\mathbf{t}_{w,y}^{t}$ are the tangent vectors to the rail and wheel surfaces at the potential contact point, respectively, $\mathbf{n}_{r}^{t}$ is the normal vector to the rail surface at the potential contact point and $\mathbf{d}_{wr}^{t}$ is the vector that defines the relative position of the point of the wheel with respect to the point of the rail. The first condition described by Eq.(1) ensures that the tangent vector to the rail is perpendicular to the vector defining the relative position of the point of the wheel with respect to the point of the rail. The second condition ensures that the normal vector to the rail is perpendicular to the tangent vector to the wheel (see [11] for details). The potential contact points determined with the procedure described above have to fulfill a last condition, that is, the parametric surfaces have to intersect each other. The conditions described in Eq. (1) are satisfied but there is no contact. This condition can be expressed mathematically as

$$\mathbf{d}_{wr}^{t} \cdot \mathbf{n}_{r}^{t} \leq 0 \quad (2)$$

which means that the intersection between two bodies is guaranteed only if the vectors $\mathbf{d}_{wr}^{t}$ and $\mathbf{n}_{r}^{t}$ point in opposite directions. The penetration d is given by

$$d = \|\mathbf{d}_{wr}^{t}\| \quad (3)$$

This procedure is performed for both the tread and flange region, thus allowing the detection of one contact point in each region of the wheel.

2.2. Normal contact problem

When two non-conforming bodies are compressed against each other, they will deform around the first point of contact and form a contact area. In the present model, the nonlinear Hertz contact theory [15] is used to analyze the normal contact problem. The normal contact force F_n between the wheel and rail is given by:

$$F_n = K_h \, d^{\frac{3}{2}} \quad (4)$$

where d is the penetration defined in Eq. (3) and K_h is a generalized stiffness coefficient that depends on the material properties of the bodies in contact, such as the Young modulus and the Poisson ratio, and on the curvatures of the surfaces at the contact point [16].

2.3. Tangential contact problem

In the present work, the longitudinal and the lateral creep forces are pre-calculated and stored in a lookup table, based on USETAB [17], to be later interpolated during the dynamic analysis as a function of the creepages and the semi-axes ratio of the contact ellipse.

2.4. Train-structure interaction system

In the present method, the governing equilibrium equations of the vehicle and structure are complemented with additional constraint equations that relate the displacements of the contact nodes of the vehicle with the corresponding nodal displacements of the structure. The formulation has been developed by [11] and takes into account the geometry of the wheel and rail and the behavior of the contact

[DOI: 10.22068/IJRARE.6.2.1]

interface. The train-structure problem can be expressed in a matrix form as:

$$\begin{bmatrix} \bar{\mathbf{K}} & \bar{\mathbf{D}} \\ \bar{\mathbf{H}} & \mathbf{0} \end{bmatrix} \begin{bmatrix} \Delta \mathbf{a}_F^{i+1} \\ \Delta \mathbf{X}^{i+1} \end{bmatrix} = \begin{bmatrix} \boldsymbol{\psi}(\mathbf{a}^{t+\Delta t,i}, \mathbf{X}^{t+\Delta t,i}) \\ \bar{\mathbf{r}} \end{bmatrix} \quad (5)$$

where $\bar{\mathbf{K}}$ is the current effective stiffness matrix of the vehicle-structure system, $\bar{\mathbf{D}}$ is a matrix that relates the contact forces, defined with respect to the target element coordinate system, with the nodal forces defined in the global coordinate system, $\bar{\mathbf{H}}$ is the transformation matrix that relates the nodal displacements of the target elements, defined in the global coordinate system, with the displacements of the auxiliary points defined with respect to the target element coordinate system, $\boldsymbol{\psi}$ is the residual force vector that depends on the nodal displacements **a** and on the contact forces **X** and $\bar{\mathbf{r}}$ the vector with the irregularities that may exist in the contact interface. The superscript $t+\Delta t$ indicates the current time step, while i and $i+1$ denotes the previous and current Newton iteration, respectively.

3. Safety assessment of a train running over a viaduct subjected to moderate earthquakes

3.1. Finite element model of the Alverca viaduct

The Alverca viaduct is a flyover structure belonging to the Northern Line of the Portuguese railway network that connects Lisbon to Porto. The structure comprises several simply supported spans with 21 m length supported by 10 m height columns. The deck consists of a pre-fabricated and pre-stressed U-shaped beam on which pre-slabs serving as formwork to the concrete upper slab cast *in situ* are placed, forming a single-cell box girder deck. The numerical model of the viaduct is developed in ANSYS. The deck, piers, sleepers and rails are modeled using beam finite elements, while the bearing supports, ballast and pads are modeled using linear spring-dampers. Mass point elements are also used to model the ballast mass and the non-structural elements such as safeguards and edge beams of the deck. Special focus is given to the track modeling, since it may strongly influence the behavior of the vehicle. This is one of the advantages of using the finite element method to model the structure, since in the majority of studies performed in multi-body platforms the track is considered to be rigid, which is far from reality. A schematic representation of the numerical model, along with a detail of the cross-section and the deck joint above the piers is illustrated in Figure 1 (the track is not included in Figure 1(a) for simplicity). Although the spans are disconnected from each other, the track mobilizes a certain amount of transversal stiffness when relative movements between adjacent spans occur.

As it will be explained later, the seismic actions considered in the present study correspond to moderate events with relatively high probability of occurrence. Although no significant damage to the structure is expected for these levels of intensity, a reduction in the piers' stiffness due to concrete cracking has been accounted. Thus, the effective stiffness of the piers is evaluated based on the methodology described in [14].

3.2. Finite element model of the train

As with the structure, the numerical model of the vehicle is also developed in ANSYS. The vehicle is based on a Japanese high-speed train whose properties were known. A schematic representation of the dynamic model of one of the cars is illustrated in Figure 2. The springs and dampers of the suspensions are denoted by k and c and the masses and rotary inertias are indicated by m and I. The longitudinal, lateral and vertical distances are denoted by a, b and h, respectively, Lcp refers to the lateral distance between the initial contact points and $R0$ is the nominal rolling radius. The subscripts cb, bg and ws indicate carbody, bogie and wheelset, respectively. The carbody, bogies and wheelsets are modeled using beam finite elements, while the suspensions are modeled using spring-dampers in the three directions. The masses and rotary inertias are modeled using mass point elements, located at the center of mass of each component.

3.3. Definition of the track irregularities

In the present work the track irregularities have been generated based on the stochastic Gaussian ergodic process described in [18]. Two levels of track quality have been considered: 1) regular operation limit, according to [18], with peak values of approximately 2.5 mm; and 2) alert limit defined in the EN 13848-5 [19], with peak values of approximately 4.5 mm. The profiles have been generated with 2000 discrete

[DOI: 10.22068/IJRARE.6.2.1]

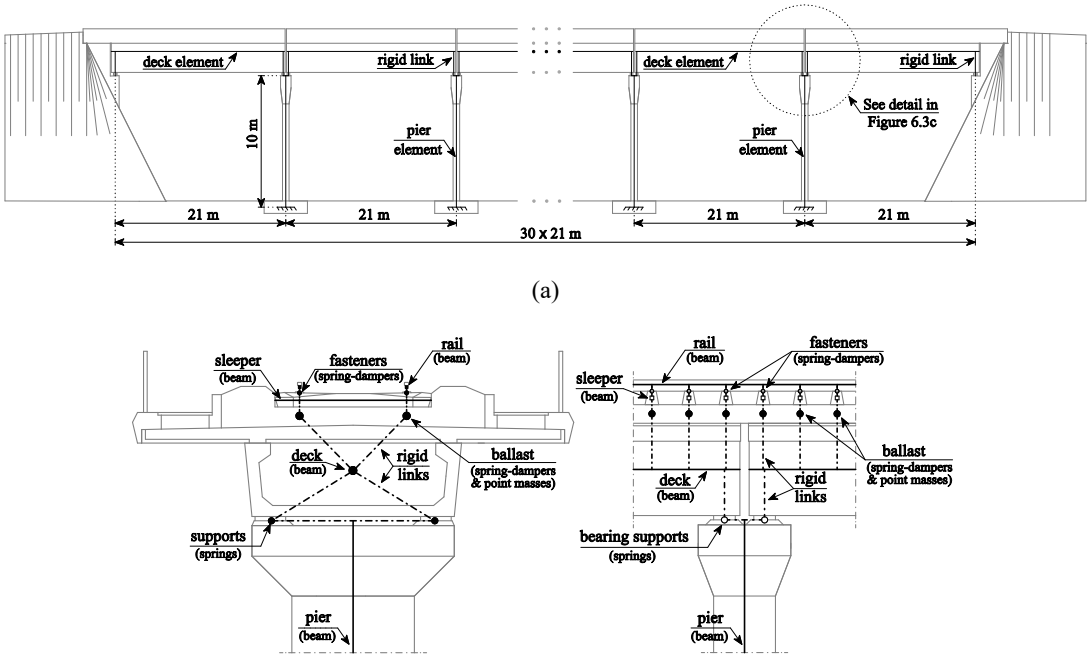

Figure 1. Numerical model of the viaduct: (a) elevation view, (b) cross-section and (c) deck joint

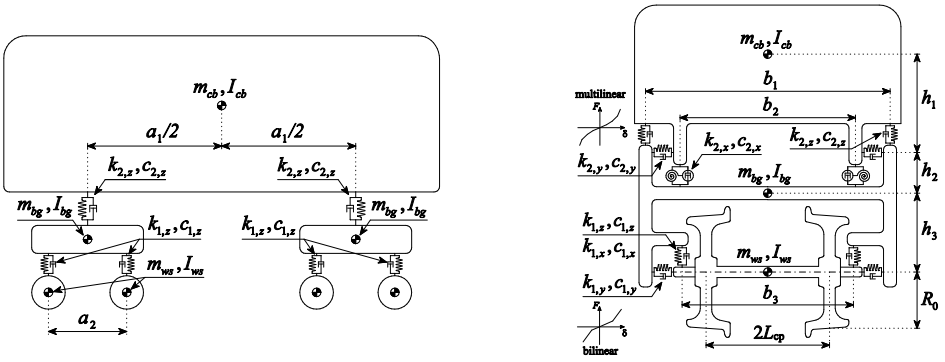

Figure 2. Dynamic model of the railway vehicle: (a) lateral view and (b) front view

frequencies with wavelengths ranging between 3 and 25 m [19].

3.4. Definition of the seismic action

The seismic excitations adopted in the present study consist of artificial accelerograms generated from the elastic spectra described in EN1998-1 [20], with PGA corresponding to moderate events with return periods less than 475 years, which is the reference return period of the design seismic action associated with the no-collapse requirement. Thus, four levels of seismic intensity with return periods of 95 (proposed return period for the damage limitation requirement of EN1998-1), 150, 225 and 310 years are considered, being the ground motion imposed along the lateral direction.

The artificial accelerograms are generated with the software SeismoArtif [21]. The target elastic spectra have been defined for the seismic zone 2.3 of the Portuguese territory and for a soil type A, with an importance factor of 1.0 (railway bridge). The PGA, provided by National Laboratory for Civil Engineering of Portugal,

[DOI: 10.22068/IJRARE.6.2.1]

corresponding to the seismic actions considered in this work are presented in Table 1. Figure 3 presents, as an example, the generated artificial ground motion with a return period of 310 years, as well as the respective response spectrum adjustment.

Table 1. PGA corresponding to the return periods of the seismic actions

Return period (years)	95	150	225	310
PGA ($m.s^{-2}$)	0.862	1.050	1.250	1.420

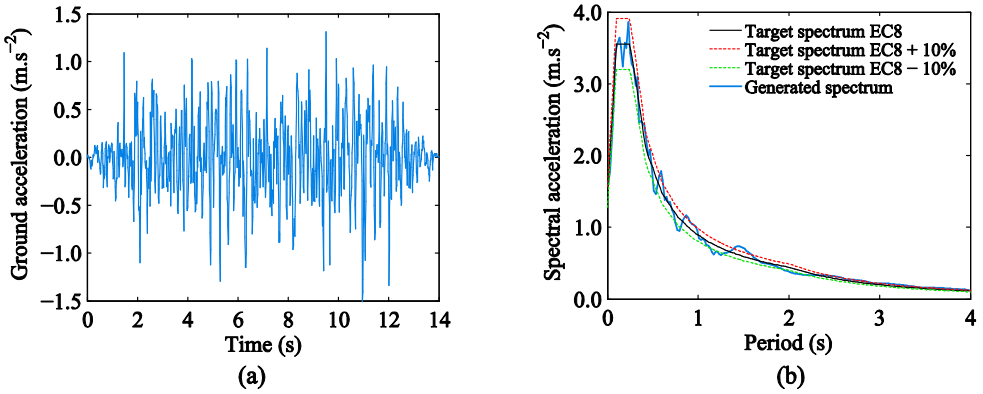

Figure 3. Generated ground motion with T = 310 years: (a) accelerogram and (b) spectrum adjustment

3.5. Running safety criteria

Three derailment criteria are used to evaluate the running safety of the train as described below. The first criterion, called Nadal criterion is defined as the ratio of the lateral Y to the vertical Q contact forces of a wheel [22]. The Nadal factor ξ_N is therefore expressed as:

$$\xi_N = \frac{Y}{Q} \tag{6}$$

The Nadal factor in any wheel of the train should not exceed 0.8 [22]. The second criterion is the Prud'homme criterion that is also defined in [22], being the Prud'homme factor ξ_P expressed in a dimensionless form as:

$$\xi_P = \frac{\sum_{ws} Y}{10 + \frac{2Q_0}{3}\,[\text{kN}]} \tag{7}$$

where Q_0 is the static load per wheel in kilo Newtons. This factor in any wheelset of the train should not exceed 1.0 [22]. Finally, the unloading criterion is defined in [23] and is related to the most critical bogie. The criterion is analyzed through the unloading factor ξ_U that is given by

$$\xi_U = 1 - \frac{Q_i + Q_j}{2Q_0} \tag{8}$$

where Q_i and Q_j are the vertical contact forces of the unloaded wheels from the wheelsets i and j from the same bogie. This factor should be limited to 0.9 [23].

3.6. Results of the running safety study

To analyze the influence of the seismic intensity in the train's running safety the maximum values of the safety criteria obtained for each seismic intensity level in a scenario in which the vehicle crosses the viaduct at 350 km/h with a track quality corresponding to the regular operation limit are presented in Table 2. While the Nadal and Prud'homme criteria, which depend on the Y/Q ratio and on the lateral contact force, respectively, are significantly affected by the earthquake, the wheel unloading criterion, which depends exclusively on the vertical contact forces, shows a lesser variation.

[DOI: 10.22068/IJRARE.6.2.1]

Table 2. Maximum values of the safety criteria for different seismic intensities

Seismic level	Unloading	Prud'homme	Nadal
No earthquake	0.72	0.37	0.26
T = 95 years	0.76	0.89	0.71
T = 150 years	0.82	1.17	0.70
T = 225 years	0.89	1.35	1.02
T = 310 years	0.89	1.42	1.05

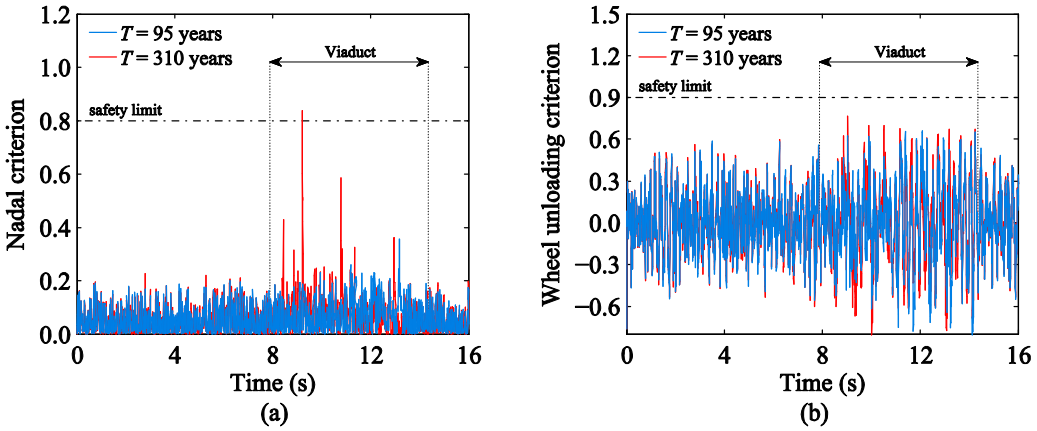

Figure 4. Safety criteria for the left wheel of the second wheelset in a scenario with V = 350 km/h and track quality corresponding to the regular operation limit: (a) Nadal and (b) wheel unloading

This is due to the fact that only the lateral component of the earthquake is accounted.

The Nadal and wheel unloading criteria obtained for the left wheel of the second wheelset for the minimum and maximum intensities are plotted as an example in Figure 4. As it can be observed, the Nadal criterion is significantly dependent on the seismic action when the vehicle is crossing the viaduct, while the wheel unloading criterion is barely affected. In order to evaluate the influence of train's speed in its safety, the maximum values of the running safety criteria obtained for vehicle speeds ranging from 200 km/h to 350 km/h in a scenario with a track quality corresponding to the alert limit and an earthquake action with a return period of 150 years are shown in Table 3. It can be observed that the vehicle speed has an important influence in both the vertical and the lateral dynamics, since the maximum values of all the criteria significantly increase with the speed.

Table 3. Maximum values of the safety criteria for different running speeds

Speed (km/hr)	Unloading	Prud'homme	Nadal
200	0.88	0.90	0.75
250	0.89	0.95	0.82
300	0.90	0.97	0.95
350	1.00	1.68	2.64

[DOI: 10.22068/IJRARE.6.2.1]

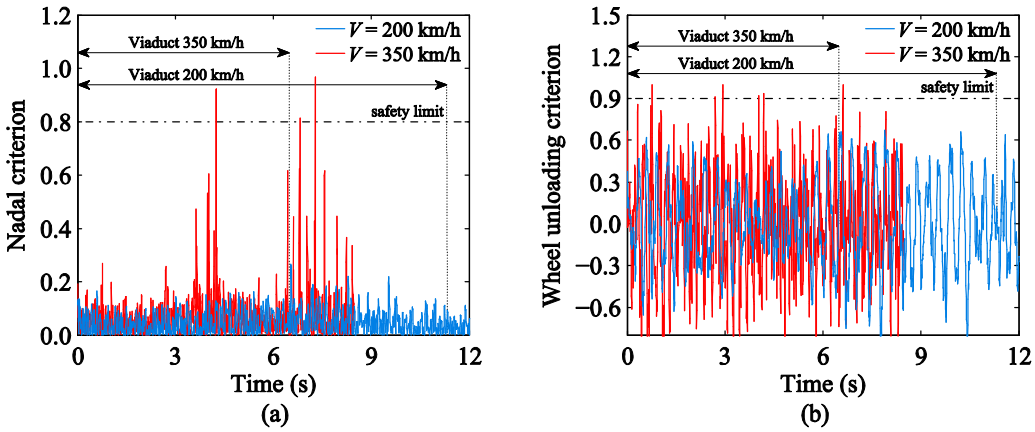

Figure 5. Safety criteria for the left wheel of the first wheelset in a scenario with an earthquake with T = 150 years and track quality corresponding to the alert limit: (a) Nadal and (b) wheel unloading

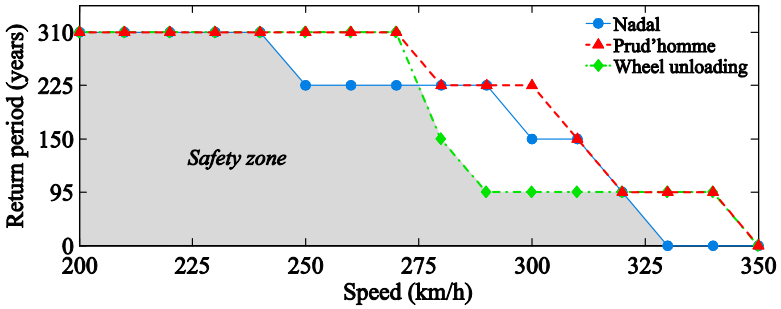

Figure 6. Running safety charts obtained for the alert limit level of irregularities

Figure 5 shows the Nadal and wheel unloading criteria obtained for the left wheel of the first wheelset when the vehicle is running at 200 km/h and 350 km/h. It is clear that both the lateral and the vertical dynamics are affected by the running speed of the vehicle. The global envelope of each of the analyzed safety criterion, as function of the running speed of the vehicle and of the seismic intensity, calculated for the alert limit level of irregularities, is plotted in Figure 6. Each point corresponds to the maximum seismic intensity that guarantees the safety of the vehicle for each running speed. As expected, the tendency observed in all the criteria is similar, indicating that the risk of derailment increases with the increasing of the speed and seismic intensity.

4. Safety assessment of a train running over a bridge subjected to crosswinds

4.1. Numerical model of the Volga River high-speed railway bridge

The present study is focused on one of the main bridges of the Moscow-Kazan HSR link, the Volga River Bridge, located near the city of Kazan (see). Due to the high levels of wind in the region (gusts up to 130 km/h), it is of the utmost importance to analyze the train running safety when it crosses the bridge at the operating speed of 350 km/h. The structure is a prestressed concrete bridge with four continuous spans of 98 + 2×190 + 98 m, as shown in Figure 7. The deck consists of a cast-in-place single-cell box girder with 6200 mm width and height ranging from 5000 mm at the middle of each span to 12500 mm over the main piers. The middle pier is monolithically connected to the deck, while the remaining piers are connected through bearing supports. The platform at the top of the deck consists of a slab with 13800 mm width which supports two ballasted tracks.

[DOI: 10.22068/IJRARE.6.2.1]

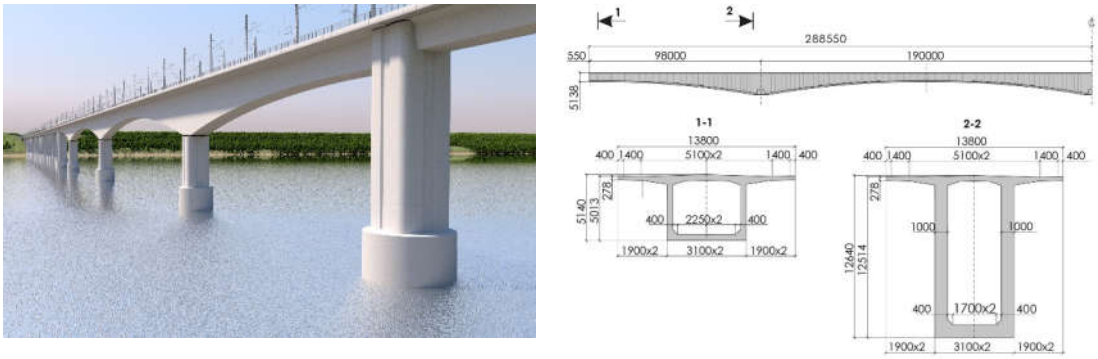

(a) (b)

Figure 7. Prestressed concrete solution: (a) photomontage and (b) elevation view and cross-sections

The numerical model has been developed with the software ANSYS. The deck, pier and rails have been modeled using beam finite elements, while ballast and pads have been modeled using linear spring-dampers. Mass point elements have been also used to model the ballast mass and other non-structural elements. The connections between the top of the middle pier and the deck and between the deck and the track have been accomplished using rigid frame elements.

4.2. Numerical model of the train

Due to the lack of data regarding the train that will run in the future HSR network in Russia, the same train described in the previous study (see Section 3.2) has been used.

4.3. Chinese Hat wind model

In the present work, the Chinese Hat model proposed in the EN14067-6 [23] is adopted to define the wind load. The gust generated in this method has a fixed amplitude (corresponding to a probability level of amplitude ~ 99 %) and a probability level of exceedance of 50 % for the gust duration (see EN14067-6 [23] for details of the wind model). The drag $F_{d,v}$ and lift $F_{l,v}$ wind forces, as well as the moment $M_{m,v}$ acting on the vehicle are given by:

$$F_{d,v} = \frac{1}{2}\rho\, V_r^2\, C_{d,v}(\alpha,\beta)\, A_v \qquad (9)$$

$$F_{l,v} = \frac{1}{2}\rho\, V_r^2\, C_{l,v}(\alpha,\beta)\, A_v \qquad (10)$$

$$M_{m,v} = \frac{1}{2}\rho\, V_r^2\, C_{m,v}(\alpha,\beta)\, A_v\, H_v \qquad (11)$$

where V_r is wind speed relative to the train, ρ is the air density, $C_{d,v}(\alpha, \beta)$, $C_{l,v}(\alpha, \beta)$ and $C_{m,v}(\alpha, \beta)$ are the aerodynamic drag, lift and moment coefficients, respectively, that depend on the attack and yaw angles, and A_v and H_v are the windward area and height of the vehicle, respectively. Similar expressions are used to define the wind forces acting on the bridge.

4.4. Results of the running safety study

The same safety criteria previously described in Section 3.5 have been used in the present study. The dynamic analyses have been performed for train speeds ranging from 200 km/h to 420 km/h. Based on the data obtained from the meteorological stations nearby the construction, the maximum wind speed consisted in 34 m/s, which corresponds to a mean wind speed, according to the Chinese Hat gust model, of approximately 20 m/s (see [23]). In all the analysis, the wind speed starts to rise from zero to the mean speed when the train enters the bridge and falls to zero again when the train leaves the bridge. It is assumed that the gust peak occurs at the midspan of the third span in the bridge. Regarding the track quality, the alert limit level previously define is Section 3.3 is adopted.

The extreme scenario corresponding to the maximum mean wind speed of $\overline{U} = 20$m/s acting on the train when it crosses the bridge at the design speed of $V_v = 420$ km/h is analyzed in Figure 8 and Figure 9. It is clear that the train reaches a limit situation where the wheels loose contact with the rail, leading to a probable overturning derailment. It can be observed in Figure 8 that the vertical contact force of the right wheel (windward side) drops to zero during

[DOI: 10.22068/IJRARE.6.2.1]

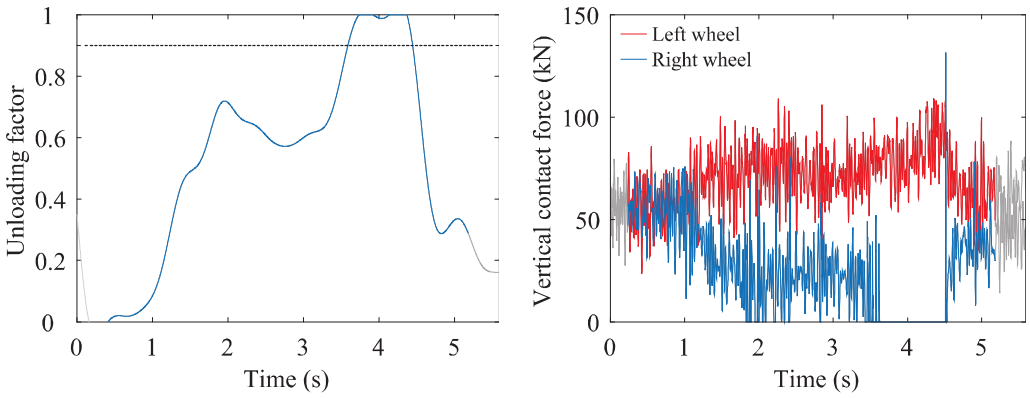

(a) (b)

Figure 8. Extreme scenario evaluation ($\bar{U} = 20$m/s and $V_v = 420$ km/h): (a) unloading criterion and (b) vertical contact forces

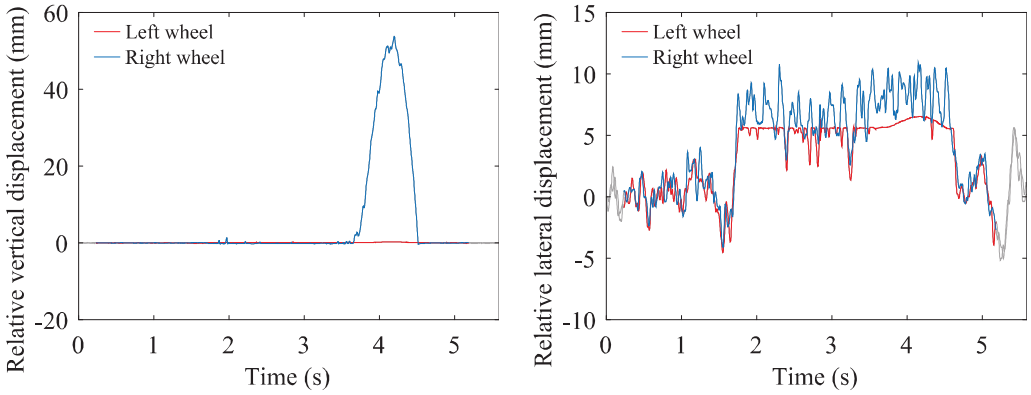

(a) (b)

Figure 9. Relative displacements between wheel and rail in the extreme scenario ($\bar{U} = 20$m/s and $V_v = 420$ km/h): (a) vertical and (b) lateral displacements

the gust peak but it suddenly reaches 130 kN on $t \approx 4.5$ s due to the reattachment impact.

By observing Figure 9, it is interesting to notice that the windward wheel jumps around 50 mm from the rail, while the 6 mm gap that exists between the rail and the flange of the leeward wheel closes between $t \approx 1.7$ s and $t \approx 4.7$ s. During this time interval, the rail is subjected to an almost constant impact with the wheel flange. This extreme scenario clearly demonstrates the importance of limiting the unloading criterion to 0.9 in order to avoid wheel detachments that can lead to overturning derailments during the occurrence of crosswinds. The crosswind stability of trains can be evaluated by analyzing the critical wind speeds that the rolling stock can withstand before exceeding some of the running safety criteria limits. The boundary between the safe and unsafe zones is therefore defined by the most critical criterion for each of the analyzed combinations of train and wind speed.

Figure 10 presents the running safety chart for the present case study, including the information of the safety criterion that is controlling the safety boundary. By observing these charts, it is possible to conclude that the train safety is significantly dependent on both the train and wind speeds. For train speeds above 300 km/h, since the lateral impacts between wheel and rail become more important due to the lack of quality of the track, the Prud'homme criterion starts to control the safety boundary.

[DOI: 10.22068/IJRARE.6.2.1]

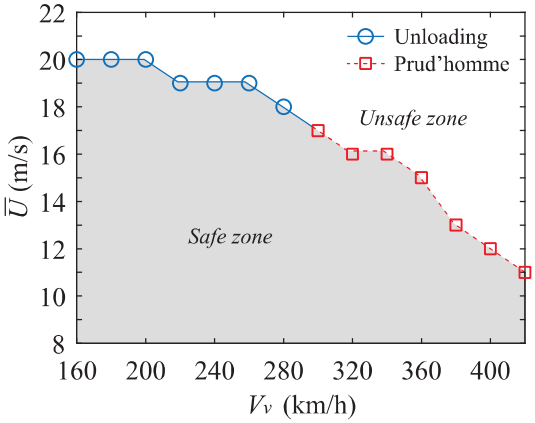

Figure 10. Running safety chart for a track quality corresponding to the alert limit level

5. Conclusions

The present paper presents a vehicle-structure interaction methodology for analyzing risk of derailment of trains subjected to lateral loads. The methodology is applied in two different case studies related to lateral dynamics.

The first case study consists of the running safety evaluation of a train moving over a viaduct subjected to moderate earthquakes. This type of events, although do not pose a significant threat to the structure, may jeopardize the stability of the vehicle and, consequently, to the safety of the passengers. Nevertheless, although the columns do not experience significant damage for these levels of seismic intensity, a reduction in their stiffness due to concrete cracking is included. The results have shown that, even for the moderate seismic intensities considered in the present study, the train safety is put at risk in a considerable number of scenarios. These results prove the importance of taking low intensity earthquakes into account in the design of railway bridges.

Regarding the second case study, in which the train running safety against crosswinds is evaluated, the results showed that the train is not prepared to run at the expected design speed of 420 km/h in safe conditions for the levels of wind that are expected to occur in the region where the Volga River Bridge will be built. For the design speed of 420 km/h, the train can withstand winds with mean speeds of 9 m/s, which is way below the maximum mean wind speed of 20 m/s considered in the study. On the other hand, if the maximum wind speed occurs, the train can safely travel over the bridge only at 200 km/h. In order to guarantee safe conditions to the train when crossing the bridge at the desired operating speed, the railway infrastructure managers should therefore install wind monitoring systems to manage the train speed depending on the weather conditions or install wind barriers in the bridge in order to significantly decrease the wind load acting directly on the train.

References

[1] C. Baker, F. Cheli, A. Orellano, N. Paradot, C. Proppe, D. Rocchi, Cross-wind effects on road and rail vehicles, Vehicle System Dynamics, 47, (2009), pp.983-1022. DOI:10.1080/00423110903078794.

[2] X. Lei, NA. Noda, Analyses of dynamic response of vehicle and track coupling system with random irregularity of track vertical profile, Journal of Sound and Vibration, 258, (2002), pp. 147-165. DOI:10.1006/jsvi.2002.5107.

[3] A. Mosleh, P. Alves Costa, R. Calçada, A new strategy to estimate static loads for the dynamic weighing in motion of railway vehicles, Proceedings Inst. of Mech. Eng., Part F: Journal of Rail and Rapid Transit, (2019), pp.1-18. DOI:10.1177/0954409719838115.

[4] H. Xia, W. Guo, X. Wu, YL. Pi, MA. Bradford, Lateral dynamic interaction analysis of a train–girder–pier system, Journal of Sound and Vibration, 318, (2008), pp.927-942. DOI:10.1016/j.jsv.2008.05.002.

[5] W. Zhai, K. Wang, C. Cai, Fundamentals of vehicle-track coupled dynamics, Vehicle System Dynamics, 47, (2009), pp.1349-1376. DOI:10.1080/00423110802621561.

[6] K. Nishimura, Y. Terumichi, T. Morimura, K. Sogabe, Development of vehicle dynamics simulation for safety analyses of rail vehicles on excited tracks, Journal of Computational and Nonlinear Dynamics, 4, (2008), no.011001. DOI:10.1115/1.3007901.

[7] M. Tanabe, H. Wakui, Sogabe, N. Matsumoto, K. Gotou, Y. Tanabe, Computational model for a high speed train running on the railway structure including derailment during an earthquake, Advanced Materials Research, 579, (2012), pp.473-482. DOI:10.4028/www.scientific.net/AMR.579.473

[DOI: 10.22068/IJRARE.6.2.1]

[8] JM. Olmos, MA. Astiz, Non-linear vehicle-bridge-wind interaction model for running safety assessment of high-speed trains over a high-pier viaduct, Journal of Sound and Vibration, 419, (2018), pp.63-89. DOI:10.1016/j.jsv.2017.12.038.

[9] T. Zhang, H. Xia, WW. Guo, Analysis on running safety of train on bridge with wind barriers subjected to cross wind, Wind and Structures, 17, (2013), pp. 203-225. DOI:10.12989/was.2013.17.2.203.

[10] SGM. Neves, PA. Montenegro, AFM. Azevedo, R. Calçada, A direct method for analyzing the nonlinear vehicle–structure interaction, Engineering Structures, 69, (2014), pp. 83-89. DOI:10.1016/j.engstruct.2014.02.027.

[11] PA. Montenegro, SGM. Neves, R. Calçada, M. Tanabe, M. Sogabe, Wheel-rail contact formulation for analyzing the lateral train-structure dynamic interaction, Computers & Structures, 152, (2015), pp.200-214. DOI:10.1016/j.compstruc.2015.01.004.

[12] MATLAB®. Release R2018a, The MathWorks Inc., Natick, MA, USA; 2018.

[13] ANSYS®. Academic Research, Release 19.2, ANSYS Inc., Canonsburg, PA, USA; 2018.

[14] PA. Montenegro, R. Calçada, N. Vila Pouca, M. Tanabe, Running safety assessment of trains moving over bridges subjected to earthquakes, Earthquake Engineering and Structural Dynamics, 45, (2016), pp.483-504. DOI:10.1002/eqe.2673.

[15] H. Hertz, Ueber die Berührung fester elastischer Körper [On the contact of elastic solids], Journal für die reine und angewandte Mathematik, 92, (1882), pp.156-171.

[16] A. Shabana, KE. Zaazaa, H. Sugiyama, Railroad vehicle dynamics: A computational approach. CRC Press - Taylor & Francis Group, Boca Raton, FL, USA; 2008.

[17] JJ. Kalker, Book of tables for the Hertzian creep-force law, 2nd Mini Conference on Contact Mechanics and Wear of Wheel/Rail Systems, Budapest, Hungary; 1996.

[18] H. Claus, W. Schiehlen, Modeling and simulation of railway bogie structural vibrations, Vehicle System Dynamics, 29, (1998), pp. 538-552. DOI:10.1080/00423119808969585.

[19] EN 13848-5. Railway applications - Track - Track geometry quality - Part 5: Geometric quality assessment, CEN, Brussels; 2005.

[20] EN 1998-1. Eurocode 8: Design of structures for earthquake resistance - Part 1: General rules, seismic actions and rules for buildings, CEN, Brussels; 2004.

[21] SeismoArtif. Version 2.1, SeismoSoft, Pavia, Italy; 2013.

[22] TSI. Technical specification for interoperability relating to the infrastructure subsystem of the trans-European high-speed rail system, Official Journal of the European Union, Brussels; 2002.

[23] EN 14067-6. Railway applications - Aerodynamics - Part 6: Requirements and test procedures for cross wind assessment, CEN, Brussels; 2010.

[DOI: 10.22068/IJRARE.6.2.1]